FEATURE ARTICLE

Multi-Attribute Seismic Analysis on AVO derived parameters – a case study

Satinder Chopra, Core Lab Reservoir Technologies, Calgary, Canada and
Doug Pruden, GEDCO, Calgary, Canada

Prospecting for reservoir zones in mature trends sometimes requires unconventional exploration tools. AVO has been successfully used as a direct hydrocarbon indicator in some clastic rocks. Lately, AVO inversion for Lame parameters ($\lambda\rho$ and $\mu\rho$) has been shown to enhance identification of reservoir zones (Goodway et al, 1997). However, the overwhelming volume of data produced in AVO inversion for these parameters can make meaningful and timely interpretation a challenge. The integration of the various AVO derived attribute volumes with other non-AVO derived seismic attribute volumes can provide meaningful geological information when tied back to well data and verified as correlating with rock properties. This paper examines a case study of a 3D seismic survey in southern Alberta, Canada where a probabilistic neural network solution was employed on AVO attributes. The results were integrated with other seismic attributes to develop a more comprehensive interpretation (Pruden, 2002).

The target area is a Lower Cretaceous glauconite filled fluvial channel, deposited within an incised valley system. A 3D seismic survey was acquired in order to create a stratigraphic model, consistent with all available well control and matching the production history. The ultimate goal was to locate undeveloped potential within the gas sands. The field has been producing since the early 1980s and two of the earliest, most prolific producers have begun to water out.

As the objective was stratigraphic in nature, the seismic data were processed with the objective of preserving relative amplitude relationships in the offset domain to allow for the use of AVO attribute analysis.

Time slice animation of the processed 3D migrated volume indicated the presence of a main valley cut in the northeast corner of the survey. A Coherence Cube™ analysis of the 3D survey, figure 1a, enhanced the channel features that were evident on the well data. The data were datumed on an easily mapped Upper Cretaceous marker to remove the distortions of regional dip from time slices at the zone of interest. Figure 1a shows this horizon slice through the coherence volume at the reservoir level.

The complex trace envelope attribute is generally used for mapping lithology changes. A composite volume containing the envelope attribute superimposed on the coherence data is shown in Figure 1b. High envelope values are seen within the incised valley, however they do not provide information that separates tight lithic sands from productive Glauconite sands.

High amplitude anomalies will not necessarily be indicative of the presence of significant gas accumulations. Only a minor presence of gas is required within pore spaces of the reservoir rock to produce significant seismic amplitude effects (Toksöz et al, 1976). It has been reported (Diaz et al, 2001) that

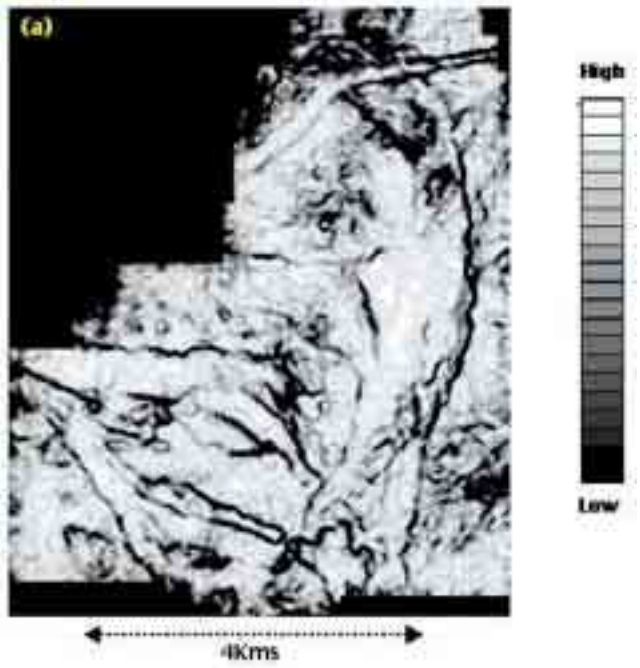

Fig 1a: A horizon slice through the coherence volume at the level of the reservoir. The definition of the main incised valley now seems quite clear.

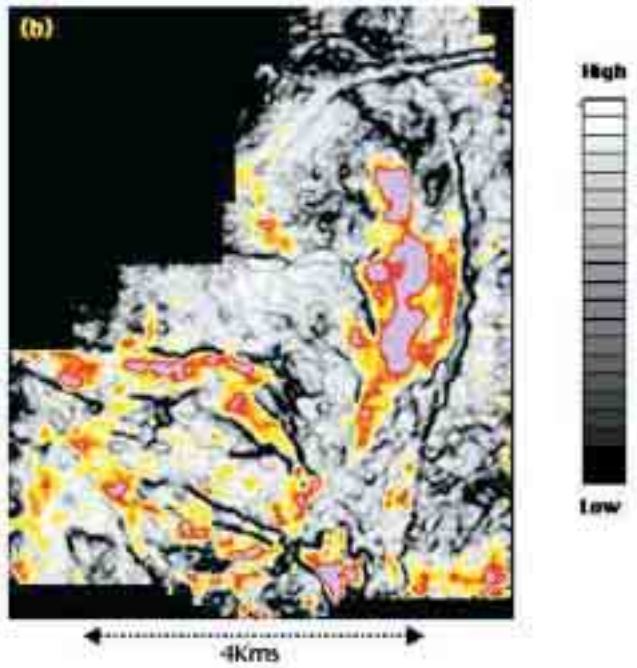

Fig 1b: A composite volume containing the complex trace envelope attribute as well as the intact coherence coefficients. High envelope amplitudes are seen within the incised valley, though, while these displays were quite revealing, they do not provide information that can separate tight lithic sands from productive Glauconite sands.

This paper was presented as a poster at the CSEG/CSPG joint convention held at Calgary from June 2-6, 2003 and it won the 'Best Geophysical Poster Award'

Continued on Page 35

Multi-Attribute Seismic Analysis on AVO derived parameters – a case study

Continued from Page 34

Glauconitic sandstone reservoir rocks can be delineated by Poisson's ratio and AVO acoustic impedance inversion analysis. The generation and calibration of synthetic seismograms with full offset stacked migrated 3D data resulted in misties suggesting the possibility of AVO effects due to lithology and pore fluid fill. The near trace stack approximates a more normal incidence model, as assumed in the synthetic seismograms, improving the well ties. From this analysis, it was determined that AVO inversion for Lamé rock parameters could provide additional insight into the geologic complexity.

AVO inversion for Lamé rock parameters

Reservoir properties can be defined in terms of fundamental rock parameters such as incompressibility and rigidity. Goodway et al, 1997 suggested Lambda-Mu-Rho analysis to extract lithology and pore fluid information from seismic and well log data. The basic theory for this analysis has been given in Burianyk, 2000, Goodway, 2001, Ma, 2001 and Dufour et al 2002.

P-wave and S-wave impedance reflectivity responses were estimated by solving the Fatti simplification of the Zoeppritz equations (Fatti et al, 1994).

$$R = \frac{1}{2}(1+\tan^2\theta)\frac{\Delta I_p}{I_p} - 4\left(\frac{V_s}{V_p}\right)\sin^2\theta$$

where $\frac{\Delta I_p}{I_p}$ = P-wave impedance reflectivity

$\frac{\Delta I_s}{I_s}$ = S-wave impedance reflectivity

The V_p/V_s ratio for the data was estimated from dipole sonic log data proximal to the area of study.

Impedance reflectivities are related to Lamé parameters of incompressibility (λ) and rigidity (μ) by the relationships $\lambda\rho = I_p^2 - 2I_s^2$ and $\mu\rho = I_s^2$ where ρ is bulk density.

The Lamé parameters cannot be directly extracted without an estimation of the density parameter ρ.

Inversion for geological parameters

AVO inversion as described above yields several seismic attribute volumes which all contain fluid and lithological information:

- Density scaled compressibility
- Density scaled rigidity
- Derived normal incidence P-wave stack
- P impedance reflectivity
- S impedance reflectivity
- Fluid factor stack (Fatti et al, 1994)

Figure 2 shows the Lambda-Rho and Mu-Rho sections with the anomaly enclosed in a yellow polygon. The cross-plots for these two attributes are also shown. The yellow dots on the cross-plots represent the values within the polygons on figures 2 a and b. The red polygon on figure 2d indicates where we would expect to find the gas sands in Lambda-Rho and Mu-Rho space. In addition to gas sand identification, significant lithological information can be derived from the data.

Multivariate statistical analysis can be used as an aid in determining whether the derived property volumes are related to gas satu-

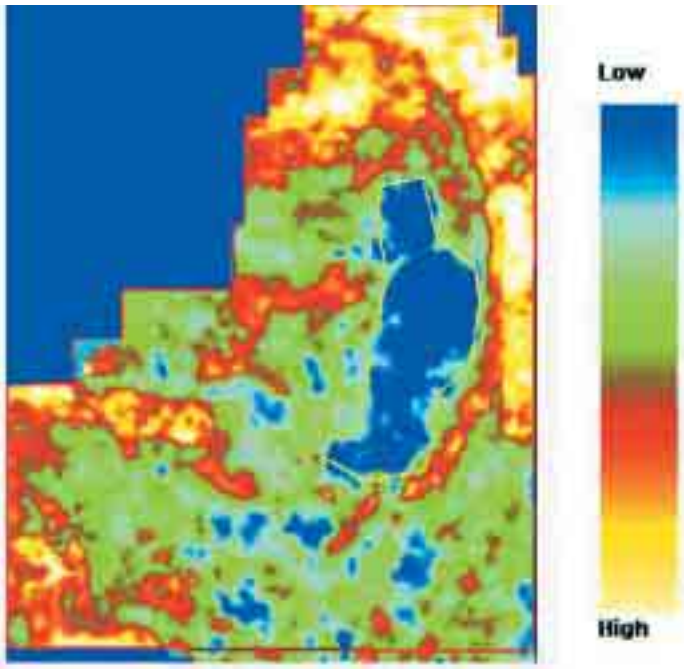

Fig 2a: Time slice from Lambda-Rho showing the suspected gas anomaly. Low values of Lambda-Rho are shown in blue.

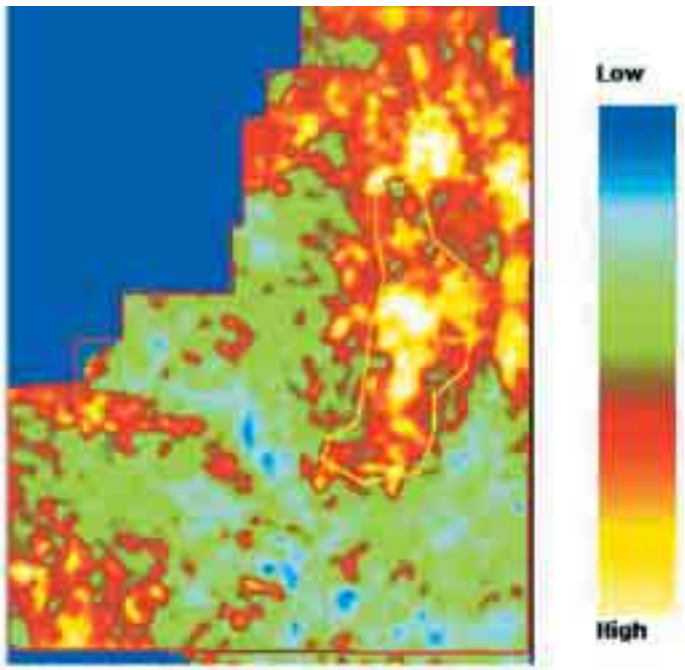

Fig 2b: Time slice from Mu-Rho showing the suspected gas anomaly showing high values of Mu-Rho in yellow and red.

Continued on Page 36

Multi-Attribute Seismic Analysis on AVO derived parameters – a case study

Continued from Page 35

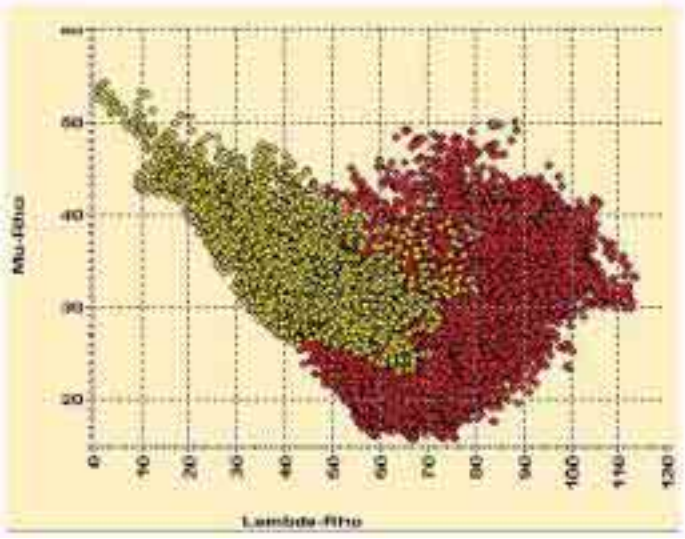

Fig 2c: Cross-plot of Lambda-Rho vs Mu-Rho. The red polygon encloses all the live data points on both the time slices. The yellow polygon encloses the suspected anomaly. The cross-plot shows the yellow points corresponding to low values of Lambda-Rho and high values of Mu-Rho which is expected of a gas anomaly.

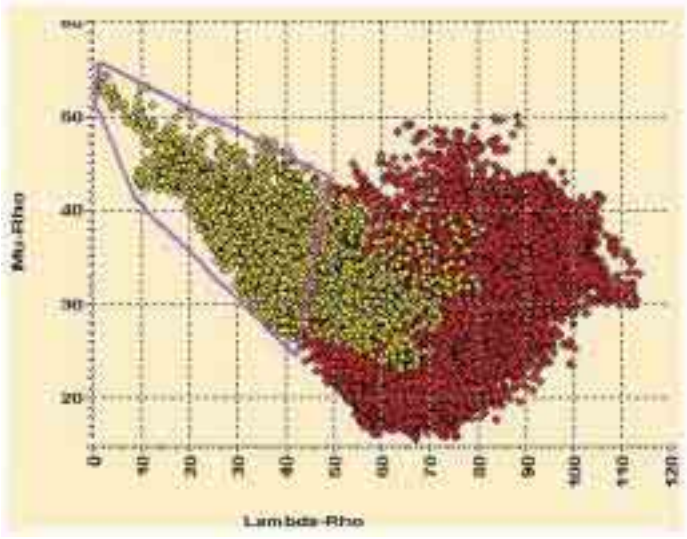

Fig 2d: The enclosed points within the purple polygon on the cross-plot represent high values of Lambda-Rho and low values of Mu-Rho. These points are highlighted on figures 2e and 2f, confirming the anomaly.

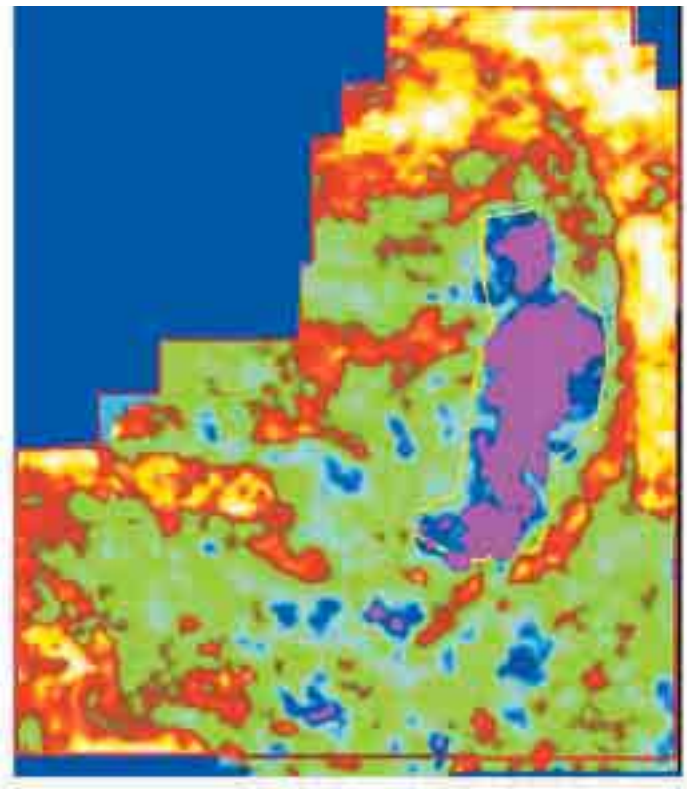

Fig 2e

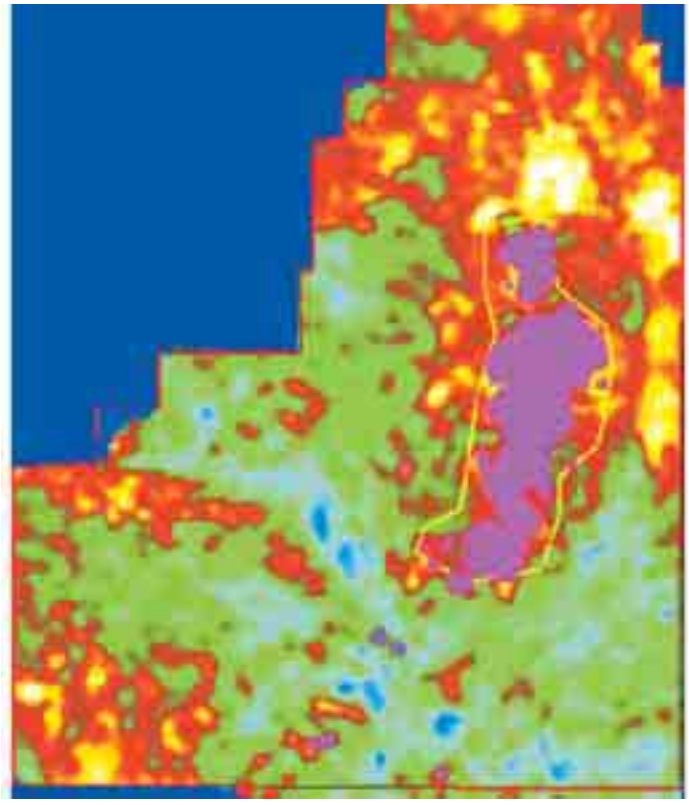

Fig 2f

ration and lithology. Our approach examines the relationship between variables to determine whether common clusters or groupings will form that represent a particular lithology or fluid fill. Figure 2. shows a two dimensional example of this approach in which gas sands tend to separate themselves in Lambda-Rho, Mu-Rho cross-plot space. This approach becomes less intuitive when more than three variables are considered simultaneously. It is difficult to visualize n-dimensional cross-plot space if n is greater than four even when color is used as a fourth dimensional separator. It is within this n > 4 space that clustering or separation of differing lithology and fluid fill may be most evident.

An example of the separation power of cluster analysis is shown in Figure 3. Within the zone of interest, the value for each of the six

Continued on Page 37

Multi-Attribute Seismic Analysis on AVO derived parameters – a case study

Continued from Page 36

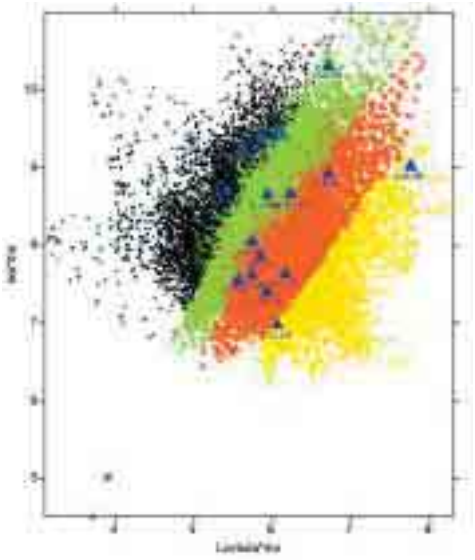

Fig 3: Lambda-Rho vs Mu-Rho cross-plot with multi-attribute cluster classifications and posted values at wells within the study area

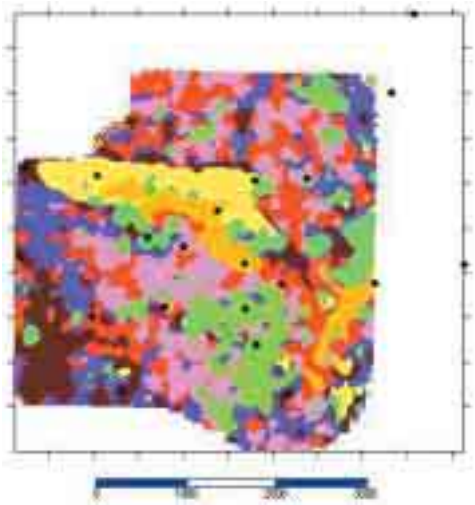

Fig 4: A subset volume of the 3D study area that has been subjected to K-means cluster analysis. Note that the analysis appears to reveal some lithological information, but the clusters have not yet been subjected to classification according to the well control.

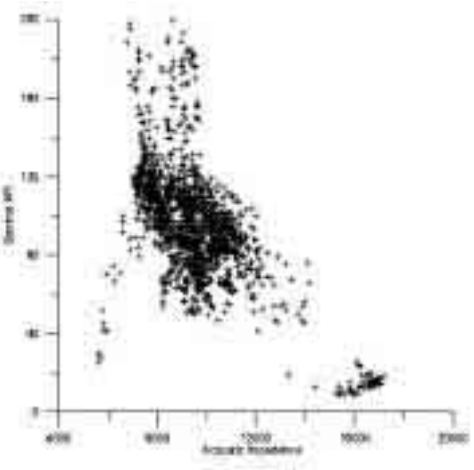

Fig 5: Cross-plot of API gamma ray values against acoustic impedance. Note the non-linear nature of the relationship.

variables has been subjected to a k-means cluster separation analysis, assuming that four distinct classes exist within the dataset. As can be seen in Figure 3, the cluster separation has divided the data into separate zones, based on the common relationships between the variables.

This type of unsupervised cluster separation analysis is often capable of creating useful character mappings of the data in 3D space by reducing a large number of attributes down to one (assigned cluster) that can be visualized on a map. Figure 4 is a small subset of the larger 3D that has had this analysis performed. Different clusters may tend to associate themselves with differing lithologies which can be verified by well data.

Analysis of this type has many inherent limitations. First, the results are sensitive to the number of clusters selected by the user. Testing is necessary in order to avoid underestimating or overestimating the number of clusters that adequately represent the data. Additionally, there is no guarantee that the derived clusters have anything to do with the lithology or fluid fill. The results must be calibrated to the well control. Thirdly, there is no guarantee that the wells have exhaustively sampled the geological space, or that the existing well control is representative of the statistical variability of the lithology.

Given that the gamma ray logs in this area are diagnostic of sands, gamma ray logs exist for each well and there is a fairly even sampling of well data across the field, a deterministic approach was found that allowed us to quantitatively relate the measured seismic attributes to the gamma ray data. A simple analysis of the relationship of gamma ray values to acoustic impedance (Figure 5) suggests that while a general relationship between the two is visually apparent, it is clearly a nonlinear relationship. Further analysis of the other attributes with the gamma ray curve produces similar results.

A nonlinear multivariate determinant analysis between the derived multiple seismic attribute volumes and the measured gamma ray values at wells is a problem ideally suited for neural networks (Hampson, et. al., 2001). By training a neural network with a statistically representative population of the targeted log responses and the multiple seismic attribute volumes available at each well, a nonlinear multiattribute transform can be computed to produce an inversion volume of the targeted log type.

Using the gamma ray, acoustic and bulk density log curves available over the zone of interest for the sixteen wells, the procedure described by both Hampson et al 2001 and Leiphart and Hart 2001 was employed to derive gamma ray and bulk density inversions across the 3D volume.

Discussion of results

The resulting gamma ray inversion is shown on the horizon slice in Figures 6a and 6b (the same slice as shown previously). The data are scaled to API gamma units in Figure 6a and converted to porosity in Figure 6b using the following standard linear density relationship (Schlumberger, 1989).

$$\rho_b = \phi\rho_f + (1 + \phi)\rho_{ma}$$

where ρ_b = bulk density

ϕ = porosity

ρ_{ma} = a clean formation of known matrix density

ρ_f = a fluid of average density

From log data, the sand filled channels are interpreted as having gamma values less than 50 API gamma units. This cutoff value was used to mask out inverted density values for silts and shales. Analysis of Figures 6a and 6b shows three distinct sand bearing

Continued on Page 38

Multi-Attribute Seismic Analysis on AVO derived parameters – a case study

Continued from Page 37

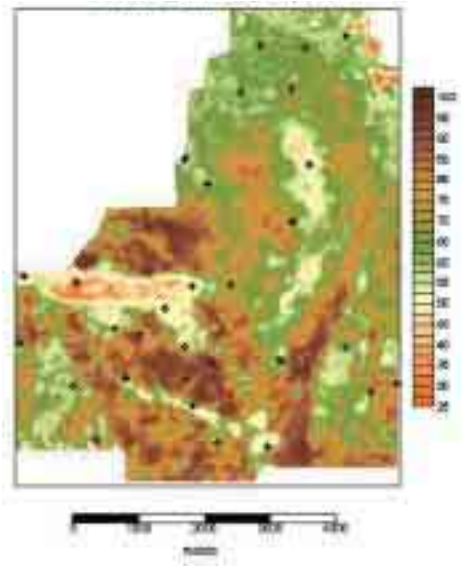

Fig 6a: Neural network inverted gamma ray response. The time slice is the same as referenced in Fig.1. Note the distinct separation of sand from silt and shale not imaged in Figure 1.

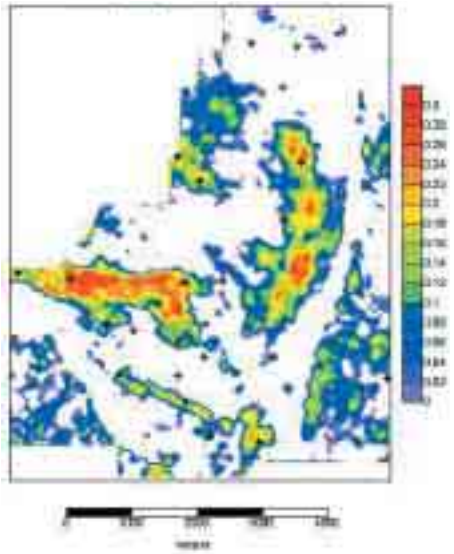

Fig 6b: Neural network computed porosity from inverted density response. The time slice is the same as referenced in Fig.1. Note the distinct separation of sand from silt and shale not imaged in Figure 1. The density values have been masked out for gamma ray values representative of silt or shale, giving a relative porosity indicator for the sands.

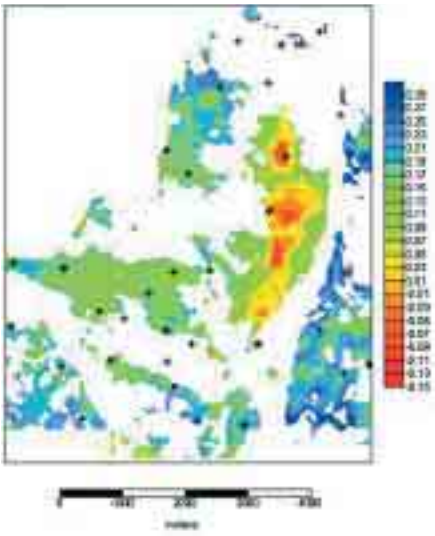

Fig 7: Computed Lambda representing relative fluid incompressibility. High values of incompressibility such as brine are colored blue, while low incompressibility is represented by red and suggest gas.

channels. The coherence time slice indicates the boundaries of the channels clearly and the gamma ray inversion helps in interpreting major sand bodies within the channels.

The incompressibility coefficient ((Lambda) was determined by dividing the Lambda rho value by the inverted bulk density. The results are represented in Figure 7. High values of incompressibility are thought to represent brine and are colored blue, with lower (more compressible) values colored green, suggesting oil or red, suggesting gas.

Analysis of the rigidity coefficient ((Mu) suggests that the sands observed within the longer, north-south trending sand body on the eastern half of the survey contain a different rock type than the sand bodies present in the west half of the survey. These results are consistent with the observed production from the two gas wells that penetrate the north-south channel. The geomorphology of this north-south channel indicates that it was deposited in a different depositional cycle than were the other channels, providing for the potential opportunity for a different lithology to de deposited.

Conclusions

AVO inversion results for the estimation of Lame parameters were successfully integrated with seismic attribute volumes derived from neural network analysis. The results were converted to volumes of log gamma ray and bulk density. These geologically meaningful parameters contributed to the estimation of relative sand distribution, porosity and fluid content estimates.

Two new drilling locations derived from this work encountered a new gas charged reservoir, extending the life of the gas pool and adding new reserves to the operating company's portfolio.

Suggested Reading

Burianyk, M., 2000, *Amplitude vs Offset and seismic rock property analysis: A primer*; CSEG RECORDER, V25, no.9, p6-16.

Diaz, E., Prasad, M., Dvorkin, J., Guiterrez, M., and Nur, A., 2001, *Rock Physics of Glauconite and Glauconitic Sandstone Reservoirs*: AAPG Bulletin, V85, No.13 (Supplement).

Dufour, J, Squires, J., Goodway, W. N., Edmunds, A. and Shook, I., 2002, *Integrated geological and geophysical interpretation case study, and Lame rock parameter extractions using AVO analysis of the Blackfoot 3C-3D seismic data, southern Alberta, Canada*; Geophysics, 67, 27-37.

Fatti,J.L., Smith,G.C., Vail,P.J., Strauss,P.J.,Levitt,P.R.1994, *Detection of gas in sandstone reservoirs using AVO analysis: A 3D seismic case history using Geostack technique*: Geophysics, 59, 1362-1376.

Goodway, W. N., 2001, *AVO and lame constants for rock parameterization and fluid detection*: CSEG RECORDER, 26, no.6, p39-60.

Hampson, D.P., Schuelke, J.S., and Querien, J.A., 2001. *Use of multiattribute transforms to predict log properties from seismic data*: Geophysics, 66, 220-236.

Leiphart, D.J. and Hart, B.S., 2001. *Comparison of linear regression and a probabilistic neural network to predict porosity from 3-D seismic attributes in Lower Brushy Canyon channeled sandstones, southeast New Mexico*: Geophysics,66,1349-1358.

Ma, X.Q., 2001 *A robust joint inversion algorithm for rock property estimation*; CSEG RECORDER, 26, no.1,p42-48.

Pruden, D. M., 2002. *Extracting meaningful geologic parameters using multiple attribute analysis on AVO derived Lamé rock parameter inversions: 3D seismic case study from southern Alberta, Canada*, Expanded abstracts, 72nd Ann. Mtg. Soc. Expl. Geophys.

Schlumberger, Inc. 1989. *Log interpretation principles/applications*: Schlumberger,I.C.

Toksoz,M.N., Cheng,C.H. and Timur,A., 1976, *Velocities of seismic waves in porous rocks*: Geophysics, 41, 621-645.

Acknowledgements

We wish to acknowledge Kicking Horse Resources Ltd. for their permission to publish the results of this study. We also wish to thank and acknowledge Wendy Ohlhauser and Rafed Kasim of Core Lab Reservoir Technologies, Calgary for their help in processing the 3D survey and AVO analysis respectively.